Desalination and Water Treatment
www.deswater.com

doi: 10.5004/dwt.2021.27154

223 (2021) 246–256
May

Study on the phosphorus desorption of sediment from the Three Gorges Reservoir in turbulence state

Wang Li[a], Bo Zu[a], Qingwei Yang[b,*], Jun Wang[c], Jiawen Li[d]

[a]*National Engineering Research Center for Inland Waterway Regulation, Chongqing Jiaotong University, Chongqing 400074, China, emails: avanlee@126.com (W. Li), zubo@cqjtu.edu.cn (B. Zu)*
[b]*Chongqing Engineering Laboratory of Environmental Hydraulic Engineering, Chongqing Jiaotong University, Chongqing 400074, China, Tel./Fax: 86-23-62652718; email: qwyang2001@cqjtu.edu.cn*
[c]*Zunyi Water Resources Service Center, Zunyi 563000, China, email: 389282446@qq.com*
[d]*Chongqing Academy of Ecology and Environmental Sciences, Chongqing 401147, China, email: 916619087@qq.com*

Received 22 October 2020; Accepted 13 February 2021

ABSTRACT

Phosphorus (P) is one of the main substances to induce the eutrophication of water. The occurrence and migration of P in water are largely affected by the sediment. Although some studies have investigated the adsorption/desorption characteristics of phosphorus by the sediment, how the change of turbulence intensity affects the sediment flocculation and thus changes the desorption characteristics of P is still unknown. Herein, a nearly turbulent multilayer grid vibration device was designed and built to study the desorption characteristics of P by the sediment under different turbulent conditions. Furthermore, the movement and variation of particle size of the sediment that occurred in the event of turbulence have been investigated based on the images collected by the image collection device. The result shows that the secondary pollution to reservoir water may be induced by the sediment in the Three Gorges Reservoir deteriorating the eutrophication in the Reservoir. The desorption flux of P will augment with the enhancing water turbulence, sediment concentration and water temperature, where the turbulent diffusion influences the desorption of P from the sediment significantly. With the increasing intensity of turbulence, more bottom sediment will be incipiently moved and suspended which will impel the desorption of P more obviously. As the intensity amplifies further, the median diameter of the sediment tends to ascend first and then descend, and the variation of particle size caused by the flocculation and deflocculation of the sediment will affect the desorption of P to some degree. However, the dominant factor for the desorption of P is still the hydrodynamic condition, that is, the desorption of P elevates the increasing intensity of turbulence.

Keywords: The Three Gorges Reservoir; Sediment; Phosphorus; Desorption; Turbulence; Flocculation

1. Introduction

The eutrophication of water has become a worldwide major environmental problem in reservoirs, lakes and coastal zones [1,2]. The sediment is the main substance that interacts with phosphorus (P) in the water [3]. When the external pollution is controlled, the desorption of P in the bottom sediment of the reservoir area will be the main source of P in the water [4]. As an important indicator to measure the flow conditions, the intensity of turbulence has a direct impact on the state of sediment movement, the concentration of suspended sediments, and the composition of sediment particles, which plays a crucial role in the process of desorption of pollutants from the

* Corresponding author.

sediment [5,6]. However, only a few studies investigated the influence of water turbulence on the desorption of P from the sediment, and how the change of turbulence intensity affects the sediment flocculation and thus changes the desorption of P is still unknown.

The previous studies on the interaction between the sediment and the pollutants like P were mainly performed in a small oscillator with a great intensity of oscillation to sufficiently blend the sediment particles with pollutants in water [7–9]. The effects of temperature [10], pH [11] and zeta potential [12] on the adsorption/desorption of P from the sediment were studied. However, the hydrodynamic conditions in such small-scaled oscillators are far from those of the natural water. It is impossible to simulate the motion state of the sediment under the natural hydrodynamic conditions using such apparatus [13]. In addition, the sediment will show a flocculation or a deflocculation under different hydrological conditions, which has not been fully conducted up to date.

To research the movement of sediment and its effect on the absorption and desorption of pollutants involving P by sediments in water under the natural hydrodynamic conditions, many previous researchers carried out the experiments in wave flume [14], annular flume [15,16] or Plexiglass cylinder [17]. However, the flow conditions produced by the above apparatus were too simple to control the movement state of the sediment accurately. It is difficult to implement the real-time monitoring of the sediment particles, and to establish the quantitative relation between the turbulence intensity and the absorption or desorption amount of pollutants. In this research, we have developed a set of apparatus for the quasi-uniform turbulence simulation. Firstly, the desorption flux of P from the original bottom sediment in a small oscillator was carried out to assess the effect of P in the bottom sediment on the overlying water in the Three Gorges Reservoir water. Then, using the apparatus for the quasi-uniform turbulence simulation, the uniform isotropic turbulence was generated in the cylinder through the multi-layer vibrating grille to simulate turbulent flow of water with different intensities. The real-time particle observation was also established. Therefore, the moving state of sediment particles and the desorption of P under various turbulence intensities were studied to exploit the effect of flocculation and deflocculation of sediments on the desorption of P. The results in this study were essential for the adsorption/desorption of pollutants from the sediment under various hydrodynamic conditions in the Three Gorges Reservoir.

2. Materials and methods

2.1. Sediment sampling and treatment

The sediment samples were collected from the Three Gorges Reservoir Area, Changshou District, Chongqing, China (107°02′05.5″–107°05′33.5″ E, 29°47′05.1″–29°49′04.4″N) in May 2019 as the sampling points shown in Fig. 1. The waterway of Changshou District was a typical curved section of the Three Gorges Reservoir. The river bed boundary was stable with cumulative sedimentation. The sampling points were affected by various pollution sources, including transportation activities, the urban runoff and the sewage discharge from surrounding cities. After the sediment samples were retrieved, they were screened and then stored in refrigeration.

The pH of the sediment samples was measured by an in-situ soil pH meter (Veinasa-pH, Veinasa, Mianyang, China). Organic carbon, total P and total nitrogen were determined by the potassium dichromate external heating

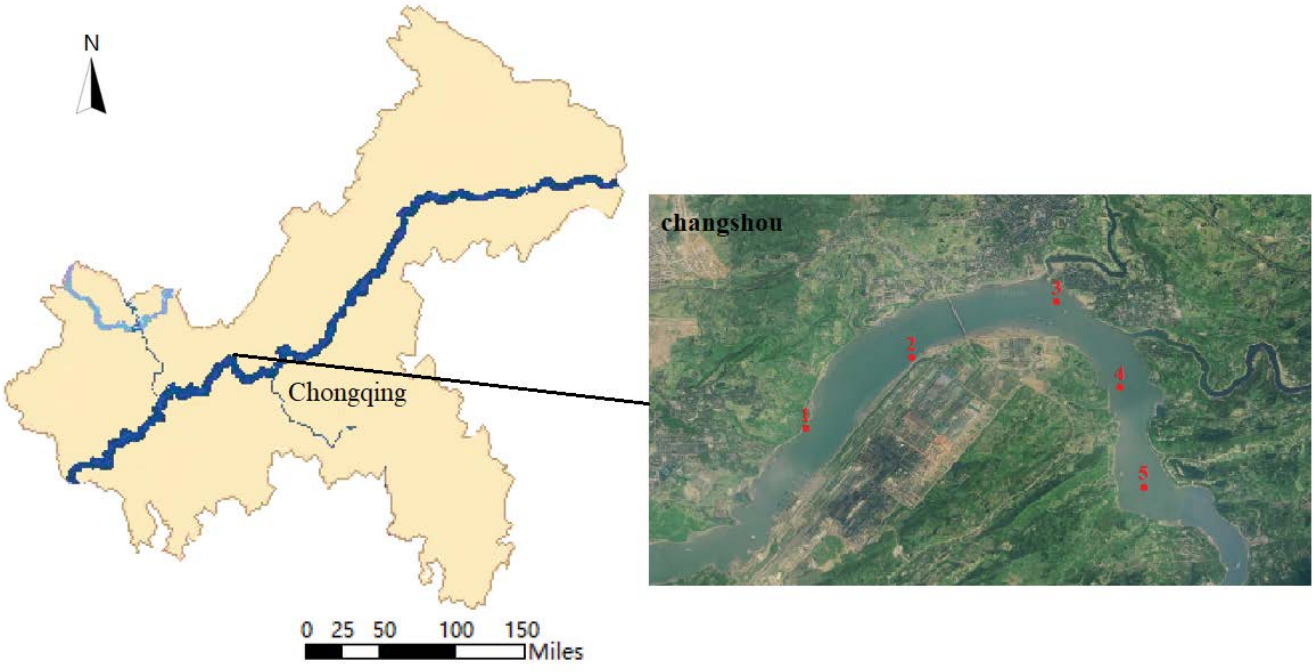

Fig. 1. Sampling points.

method, the alkali fusion-molybdenum antimony spectrophotometry and the Kjeldahl method respectively. The distribution of particle size of sediment samples was measured by a laser particle size analyzer (SALD-3101, SHIMADZU, Kyoto, Japan). The mineral compositions of sediment samples were measured by a X-ray diffractometer (XRD-6100, SHIMADZU, Kyoto, Japan). The physical and chemical characteristics of the sediment samples are shown in Table 1.

2.2. Quasi-uniform turbulence simulation apparatus

The apparatus for the quasi-uniform turbulence simulation was developed in the present study as shown in Fig. 2. This set of apparatus consisted of eight parts, such as the electric motor, the cylinder, the vibrant grille, the camera and the computer, etc. The electric motor was set at the top of the apparatus with an adjustable rotation frequency. When the motor worked, the electric motor drove the grille attached up and down to generate the turbulence. The cylinder was made of Plexiglass with a height of 200 cm, outer diameter of 30 cm and a wall thickness of 1 cm. 7 layers of grilles totally were installed in the cylinder with an interval (H = 25 cm) between each two layers. The distance of the adjacent grille hole in each grille is 5 cm with a grille porosity of 70%. These settings could produce a stable and uniform turbulence field [18]. An observation chamber of sediment particles was set at the bottom of the grille with a hole on the upper surface linking the cylinder. The sediment observation apparatus consisted of a CMOS camera, an annular LED, a crossed slid platform with high precision, a tripod and a computer were applied to record the images of sediment movements at various turbulence intensities. The particle sizes of the sediment were analyzed using the ImageJ (Fig. 3).

The turbulent intensity produced by the grilles was affected by the diameter of the cylinder, the spacing of the grille, the amplitude and frequency. Given the constant cylinder diameter and grid spacing, the turbulent shear rate could be adjusted quantitatively by changing the vibration frequency and amplitude of the grid in the experiment.

The 3D flow velocity in the grilles was measured using Acoustic Doppler Velocimeter (16 MHz, MicroADV, SonTek, San Diego, California, USA) under different conditions. The relationship of the turbulence shear rate, the amplitude,

Table 1
Physical and chemical characteristics of sediment samples

Property	Sediment samples				
	S1	S2	S3	S4	S5
pH	7.43	7.78	7.56	7.66	7.72
Total organic carbon (g/kg)	9.92	8.29	11.28	10.59	12.04
Total phosphorus (g/kg)	0.43	0.49	0.56	0.72	0.81
Total nitrogen (g/kg)	0.61	0.59	0.68	0.86	0.89
Sand (≥0.05 mm), %	4.12	3.96	3.87	3.99	1.63
Silt (0.002–0.05 mm), %	89.47	93.01	89.50	88.13	86.42
Clay (≤0.002 mm), %	6.41	3.03	6.63	7.88	11.95
Quartz, %	42.66	45.04	41.18	42.9	43.88
Potash feldspar, %	6.07	5.92	5.59	6.33	6.21
Plagioclase, %	11.52	10.12	12.07	11.47	11.19
Calcite, %	7.27	7.09	6.9	7.04	7.2
Illite, %	25.07	24.87	26.55	26.21	25.54
Chlorite, %	7.41	6.96	7.71	6.05	5.98

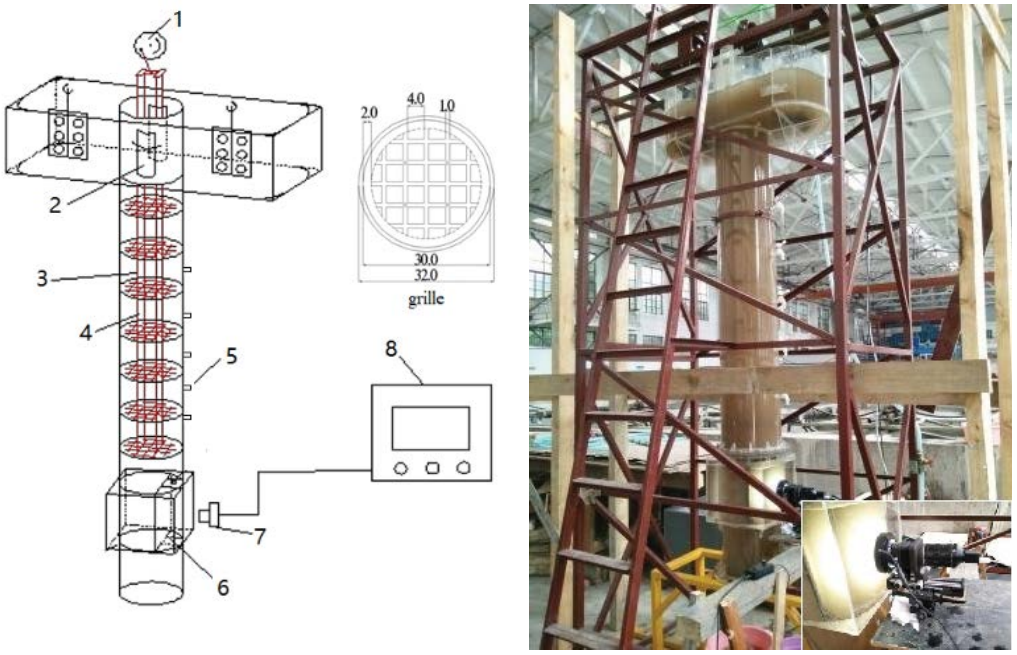

Fig. 2. Apparatus. (1) motor; (2) inlet; (3) grille; (4) grill connecting rod; (5) sampling port; (6) observation area; (7) camera; (8) personal computer.

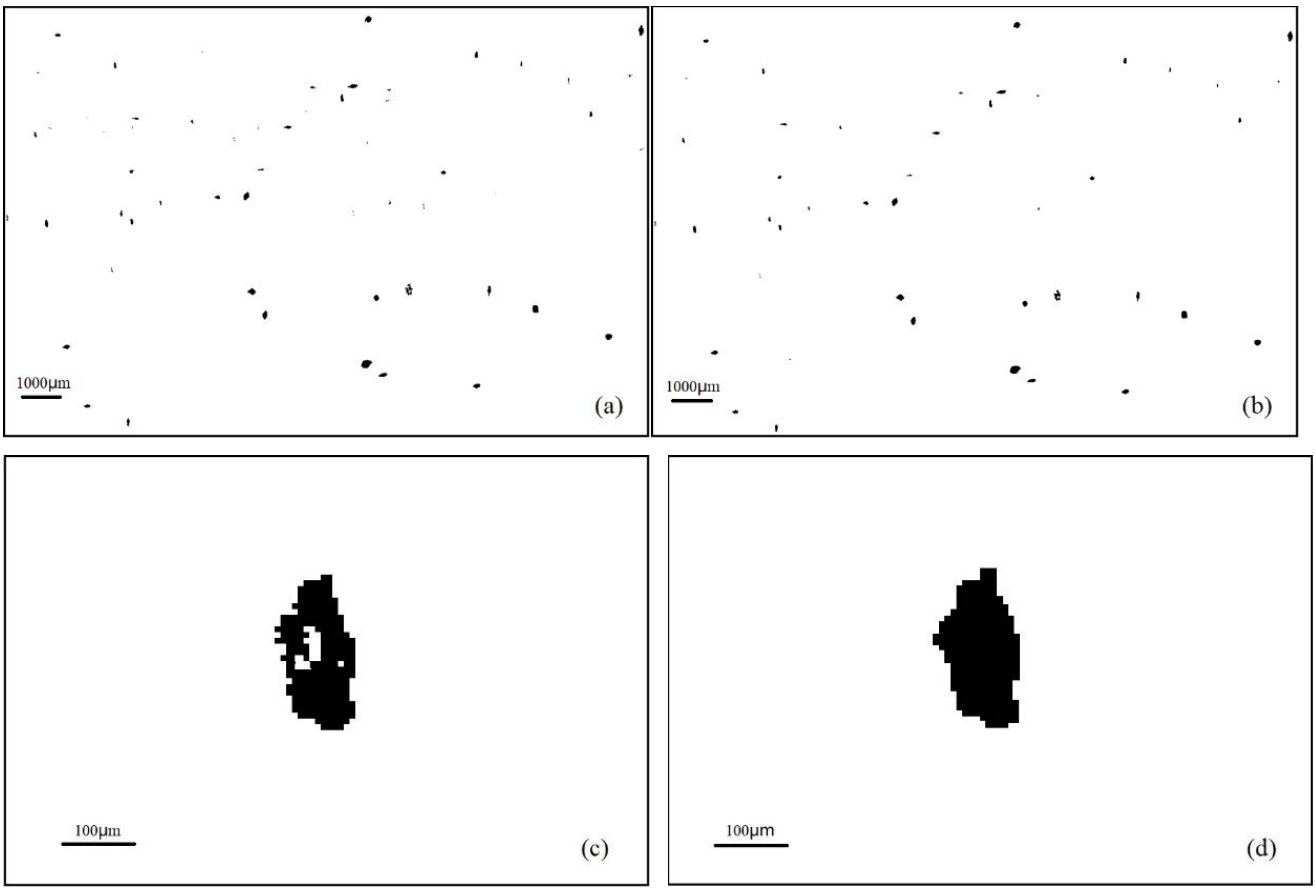

Fig. 3. Floc image: (a) binarized image, (b) noise-reduced image, (c) magnified floc image, and (d) complemented floc image.

the oscillation frequency and the operation parameters of grilles was established by setting different amplitudes and oscillation frequencies to control the turbulence intensity.

The formula of turbulence shear rate was proposed by Camp [19] as follows:

$$G = \sqrt{\frac{\varepsilon}{v}} \tag{1}$$

where G is the turbulence shear rate; ε is the energy dissipation rate of turbulence and v is the viscosity coefficient of moving fluid.

The energy dissipation rate of turbulence ε is calculated as the following formula [20]:

$$\varepsilon = A\frac{u'^3}{l} \tag{2}$$

where A represents the constant 1; the u' represents the root mean square velocity (RMS) flow in the turbulent field and the l represents the integral scale.

The following two formulas were used to calculate the RMS flow in the turbulent field u' and the integral scale l [18]:

$$\left(\frac{l}{H}\right)_{\max} \approx \begin{cases} 0.045 & S/H \le 0.15 \\ 0.25\left(S/H\right) & S/H \ge 0.20 \end{cases} \tag{3}$$

$$\begin{aligned} u' &= \mathrm{BM}^{1/2}S^{3/2}f\left(\frac{H}{2}+Z\right)^{-1} + \mathrm{BM}^{1/2}S^{3/2}f\left(\frac{H}{2}-Z\right)^{-1} \\ &= \mathrm{BM}^{1/2}S^{3/2}f\left[\frac{H}{\left(H/2\right)^2 - Z^2}\right] \end{aligned} \tag{4}$$

where the Z is the distance to the center of grille layers; B is the speed coefficient; S is the amplitude; f is frequency; H is the interval between grilles and M is the distance between the adjacent holes of grille.

According to Eq. (3), the integral scale of the apparatus was calculated to be l = 1.125 cm. If the turbulence shear rate in the center of grille layers is adapted as the approximately even turbulence shear rate, Z = 0. The result shown in follow can be known as substituting the conditions already known into Eq. (4):

$$u' = 4\mathrm{BM}^{1/2}S^{3/2}fH^{-1} \tag{5}$$

The velocity coefficient B is proportional to $(S/H)^{1/2}$ [18]. It is expressed as:

$$u' = B_m M^{1/2}S^2 fH^{-3/2} \tag{6}$$

where the B_m is the empirical coefficient.

With the ADV equipped to measure the turbulent velocity in the center of two-layered grilles at different amplitudes and frequencies, the root mean squared flow velocity was calculated and the relationship between B_m and $M^{1/2}\ S^2\ fH^{-3/2}$ was plotted. The horizontal velocity empirical coefficient B_m of 5.6081 and the vertical velocity empirical coefficient B_m of 6.8376 were obtained from the fitting line shown in Fig. 4.

Since this experiment mainly studied the vertical movement of the sediment, 6.8376 of B_m was applied as the value of the vertical velocity empirical coefficient. It is described as:

$$u' = 6.8376 \times M^{1/2} S^2 fH^{-3/2} \tag{7}$$

The amplitude S will be fixed at 3 cm. By substituting the Eq. (2) and Eq. (1) with the S and l = 1.125 cm, the relation between turbulence shear rate G and frequency f could be described as:

$$G = 10.854 \times f^{1.5} \tag{8}$$

2.3. Experimental procedures

2.3.1. Experiment on the desorption flux of P from the bottom sediment

Put the sediment in a 2.5 L brown jar with a slow addition of 2 L of deionized water, and then placed this jar in a constant temperature shaker. The disturbance intensity of samples 1–3 was 0–200 r/min, and the sediment concentration and temperature remained unchanged as 1.0 g/L and 20°C respectively. The disturbance intensity of samples 4–6 was 100 r/min and the temperature was constant at 20°C, and the sediment concentration was 0.5, 1.0 and 1.5 g/L, respectively. The disturbance intensity of samples 7–9 was 100 r/min, the sediment concentration is 1.0 g/L, and the temperature is 15°C, 20°C and 25°C respectively. All samples were shaken for 24 h under dark conditions, and then the supernatants were taken, filtered through a 0.45 μm filter membrane, and then the phosphorus concentrations in the filtrate were measured by an ammonium molybdate spectrophotometry. The arrangement of experiment groups was shown in Table 2. All experiments were repeated three times.

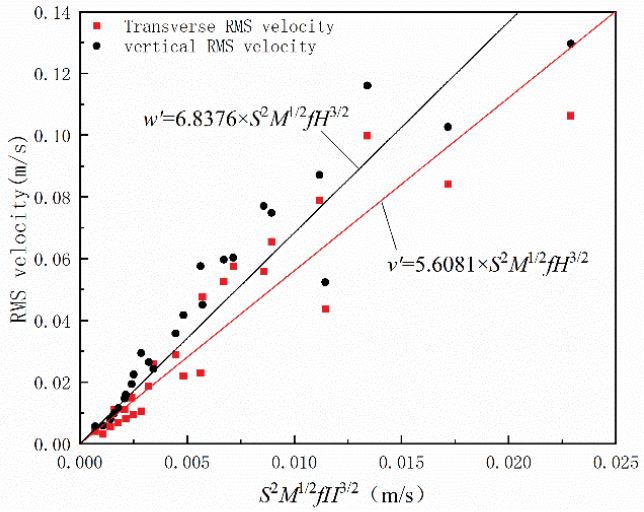

Fig. 4. Relationship between root mean square velocity and $M^{1/2}\ S^2\ fH^{-3/2}$.

2.3.2. Desorption of P from the bottom sediment at a turbulent state

The sediment was spread to the bottom of the cylinder with a thickness of 50 cm and a water temperature of 16°C. The turbulent shear rate of water flow increased from 5.04, 7.77, 14.27, 21.97, 30.70 and 40.36 s^{-1} successively with a maintenance of 120 min for each level. The sediment concentrations at the distances of 5, 25, 45, 65, 85, and 105 cm away from the bottom of the sediment were measured every 20 min. The vertical distribution of the sediment was analyzed under different turbulent states.

The contaminated sediment was used for the desorption of P. Before the desorption experiment, each group of the sediment was soaked with 2 mg/L of phosphate solution for 48 h to make it reach the adsorption saturation. The sediment was spread to the bottom of the cylindrical tube with a thickness of 50 cm and a water temperature of 16°C. The desorption experiment was divided into two groups. For the first group, the water flow shear rate was 5.04 s^{-1} in the first 120 min, then increased to 30.70 s^{-1} with a duration of 300 min, and then dropped to 5.04 s^{-1} with a duration of 300 min. For the second group, the turbulent shear rate of water flow was the same as that of the first group in the first 420 min, and then the turbulent shear rate of water flow was further increased to 40.36 s^{-1} with a duration of 300 min. 100 mL of water samples at 25 cm, 65 cm, and 105 cm were collected from the bottom sediment every 20 min. After the suction filtration through a 0.45 μm filter membrane, the contents of P in the water were measured by an ammonium molybdate spectrophotometry, and the average value was taken after three measurements.

2.3.3. Flocculation and deflocculation of suspended sediment particles and the desorption of P at a turbulence state

To explore the flocculation and deflocculation of sediment particles at various turbulent states as well as the influence of the flocculation and deflocculation on the amount of P desorbed, 6 groups of water-filled cylinders were set the suspended sediment with the corresponding turbulence shear rate of 5.04, 7.77, 14.27, 21.97, 30.70, and 40.36 s^{-1}, respectively. These turbulent shear rates kept for 3 h per stage. The HDTV camera consecutively recorded the particle images which would be binarized by the ImageJ software. The variation of particle sizes were analyzed right after the removal of error points and then the concentrations of soluble P were recorded synchronously in the experiment.

3. Results and discussion

3.1. Desorption flux of P from the bottom sediment

As shown in Fig. 5, the P in the sediment of the Three Gorges Reservoir was basically at the desorbed state under

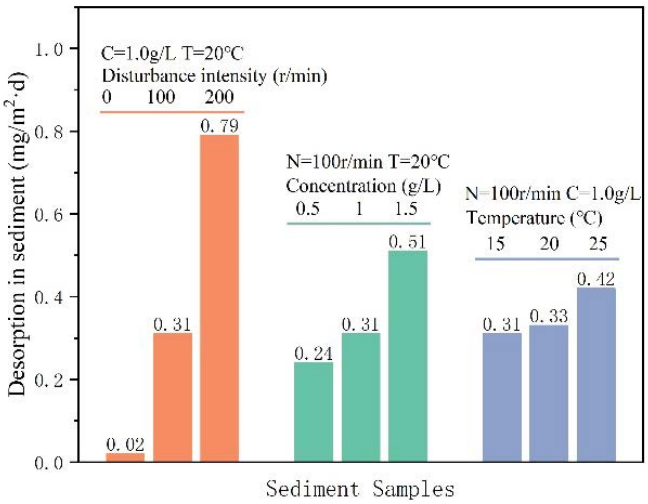

Fig. 5. The desorption flux of P from the bottom sediment.

Table 2
Desorption experiments group arrangement

Sample	Disturbance intensity (r/min)	Sediment concentration (g/L)	Temperature (°C)
#1	0	1.0	20
#2	100	1.0	20
#3	200	1.0	20
#4	100	0.5	20
#5	100	1.0	20
#6	100	1.5	20
#7	100	1.0	15
#8	100	1.0	20
#9	100	1.0	25

the conditions in this experiment, which means that the secondary pollution to reservoir water was induced by the sediment in the Three Gorges Reservoir, deteriorating the eutrophication in the reservoir. The desorption fluxes differed from the different conditions of flow velocities, concentrations and temperatures. For the first group of experiment (sample #1~#3), different intensities of disturbance induced the variation of the desorption ability of P from the sediment. In general, the enhanced disturbance would amplify the movement of bottom sediment from the river bottom, impel the contact of sediment particles with water, and increase the exchange rate between the pore water inside the bottom sediment and the overlying water, accelerating the desorption of P from the bottom sediment [21]. For the second experimental group (sample #4~#6), the total amount of desorbed P varies obvious from the sediments with different concentrations, that is, the amount of desorbed P increased with the increasing concentration of the sediment, indicating that the amount of desorbed P from the sediment in the Three Gorges Reservoir enhanced with the rising concentration of the sediment in the range from 0.5 to 1.5 g/L. For the third experimental group (sample #7~#9), the desorption flux of P ascended with the increasing temperature, which could be ascribed to the accelerating physical and chemical reactions of P [10,22], and the enhancing microbial activity, so the organic P in the sediment was transformed to be inorganic P [23]. Therefore, it was necessary to pay attention on the eutrophication of reservoir in summer because of the higher temperature of water in that season.

3.2. *Influence of the incipient of bottom sediment on the desorption of P at the turbulence state*

The change process of the suspended sediment concentration is shown in Fig. 6. In the initial stage (0–120 min), there is no significant change in the concentration of the suspended sediment at a low value of the turbulent shear rate, indicating that the turbulent shear

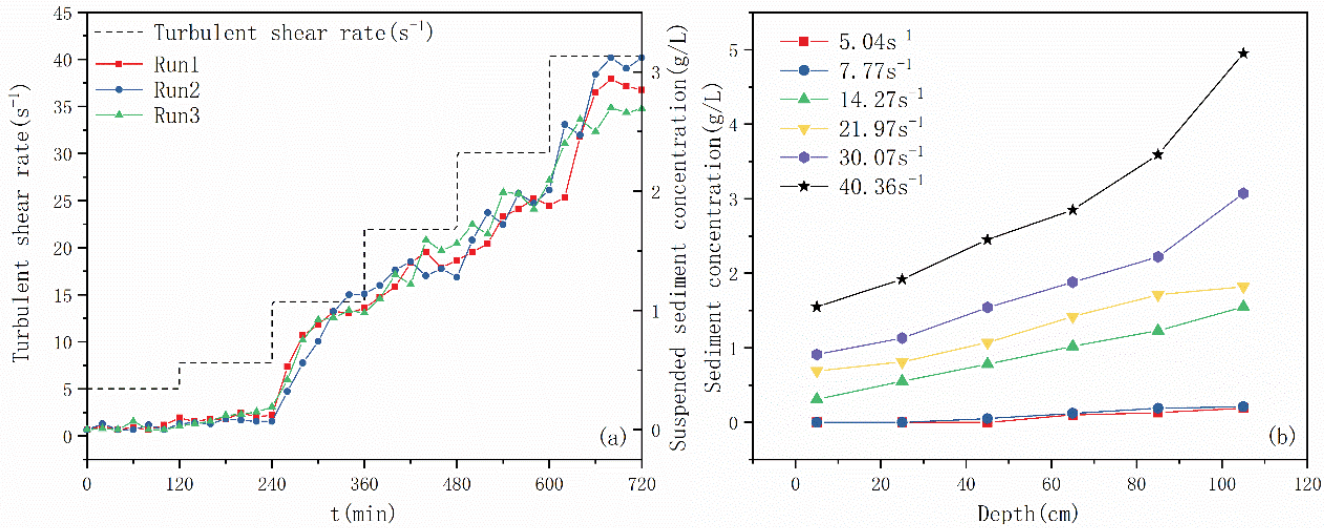

Fig. 6. Concentration of the suspended sediment and the vertical distribution of sediment.

rate did not reach the starting conditions for the incipient motion of the sediment. However, when the shear rate further increased from 7.77 to 14.27 s^{-1} at 240 min, the concentration of the suspended sediment gradually increased. Besides, it is shown that an obvious vertical gradient existed in the concentration of the sediment after the bottom sediment was triggered. The gradient was more oblique with the higher turbulence shear rate.

As shown in Fig. 7, the critical shear rate to trigger the incipient motion of the bottom sediment was not satisfied before the 120 min, resulting in no suspended sediment existed in water. The desorption of P was mainly derived from the pore water from the bottom sediment and the sediment on the surface of river bed, maintaining the concentration of P in a low level [21]. As the turbulence shear rate elevated to 30.70 s^{-1} at 120 min, the bottom sediment commonly started to move, increasing the concentration of the suspended sediment in water rapidly. Zhang et al. [24] and Zhu et al. [25] analyzed the effect of the pore water during the bed sediment resuspension process and found that the desorption of P was divided into two parts: In the initial stage of suspension, the desorption of soluble P in the pore water played a primary role. In the continuous suspension stage, the desorption mainly came from the desorption of particulate P on suspended particles. The phase of quickly desorption in the early 60 min contributed 80% of the desorbed P under such a condition. Then the system would enter the phase of desorption equilibrium after the consequently undergone a period of slowly desorption. In the first experimental group, after reaching the desorption equilibrium stage, the turbulent shear rate reduced to 5.04 s^{-1} at 420 min. As shown in Fig. 7a, the concentration of the suspended sediment dropped and the concentration of P in water descended slightly with the changing shear rate, indicating that a part of soluble P in water would be reabsorbed in the sedimentation process of the suspended sediment. In the second experimental group, the turbulence shear rate was elevated to 40.36 s^{-1} at 420 min. It can be noticed in Fig. 7b that more bottom sediment was elevated into water, and the concentration of soluble P was augmented further. Finally, the equilibrium was achieved after undergone a desorption phase in haste. It can be concluded that the incipient motion and elevation of the bottom sediment caused by the increased turbulence intensity made an obvious influence on the desorption of P. However, the desorption could also be affected by the flocculation and deflocculation from some deeper degree, which would be elaborated in following sections.

3.3. Flocculation of sediment particles and its influence on the desorption of P under the turbulence state

Under a turbulence state, the flocculation of the sediment particles occurred, which may change some physical properties of the sediment like the diameter, specific surface area and pore volume [26]. The variation of physical properties made a different influence on the absorption and desorption of pollutants. Although the influence of the particle size specificity of the suspended sediment on the absorption/desorption of P had been studied formerly [27–29], only the absorption and desorption in a static water were concerned without taking the variation of the movement of sediment particles under a natural turbulence state into concern. Furthermore, the flocculation and deflocculation also induced the variation of sediment particles under the influence of turbulence conditions. Besides, the adsorption process of P from the sediment was studied under the natural condition by the simulation apparatus with the oscillation of grilles by some researchers, presenting that a close relation existed between the adsorption ability of P and the adsorption efficiency of P from the sediment and the particle size of sediment, concentration of sediment had been concluded [30]. For compensation, some have proposed the influence of amplified intensity of turbulence on accelerating the matter exchange between the sediment and water, which causes the desorption of P [31]. Whereas, the variation of properties of the sediment induced by the turbulence was not considered.

Fig. 8 shows the variation of particle sizes under different turbulence shear rates. Among the 6 groups set in

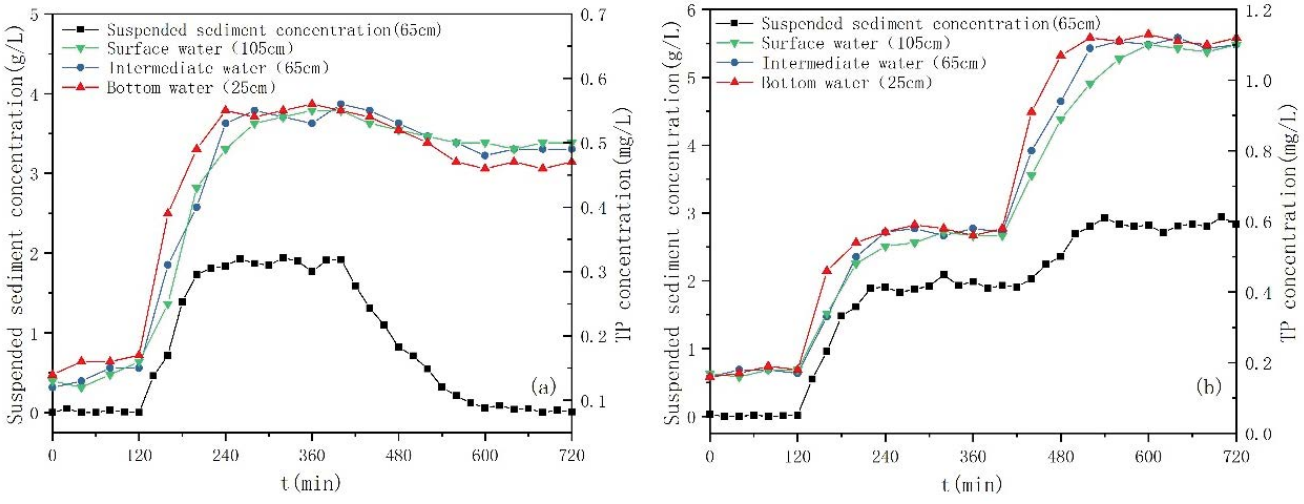

Fig. 7. Change of suspended sediment concentration and P desorption in turbulence flow.

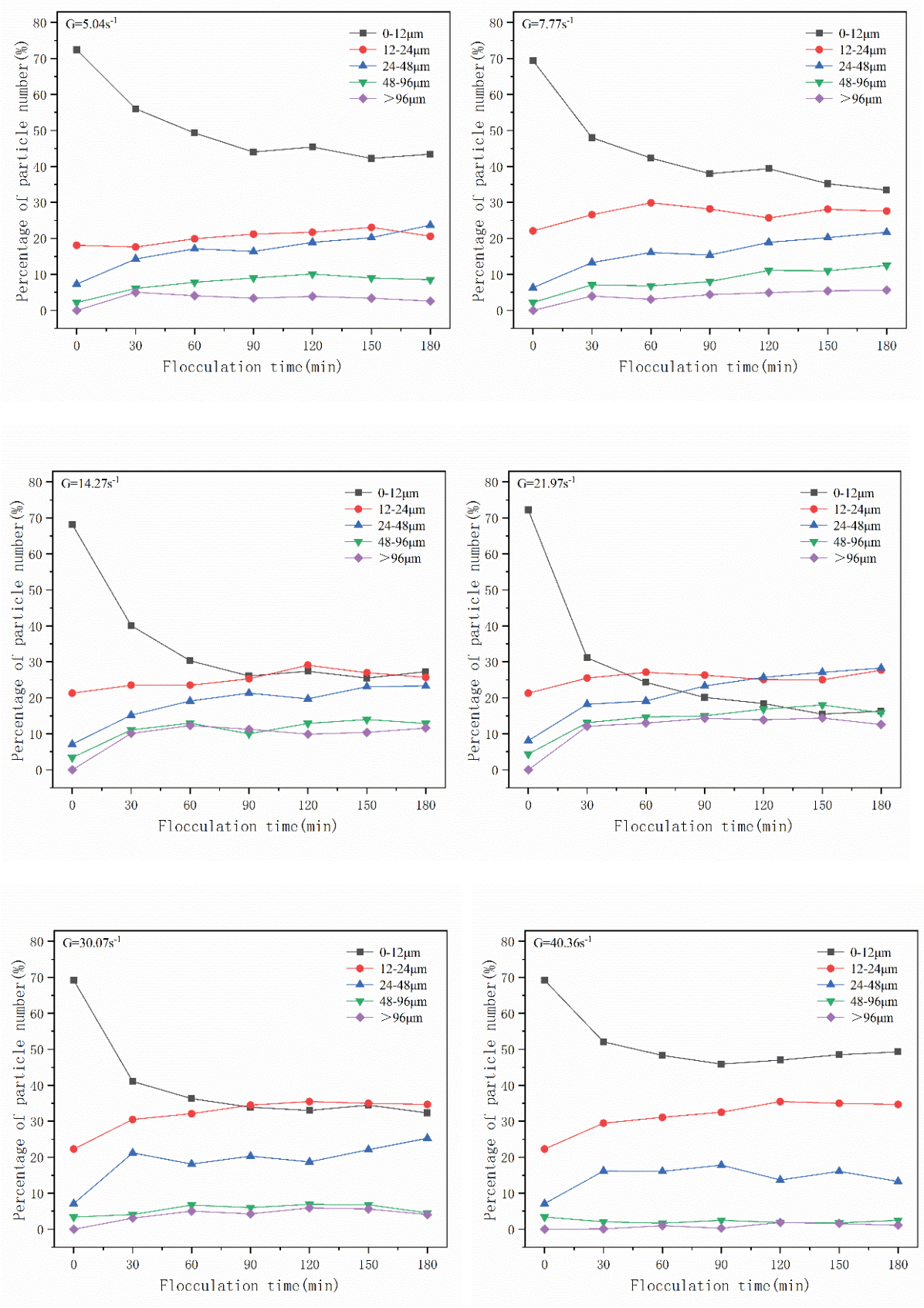

Fig. 8. The variation of particle sizes under different turbulence shear rates.

the experiment with different shear rates, the sediment collected from the Three Gorges Reservoir was able to flocculate to different degrees, where the proportion of the sediment of small particle size with a diameter range of 0~12 μm decreased while the proportion of sediment of big particle size increased. Many tiny particles aggregated with each other to form flcos. However, the performances of the flocculation of the sediment varied from the different turbulence shear rates. When the shear rate was under the level of 21.97 s^{-1}, the proportion of sediment particles of small sizes with a diameter ranging from 0 to 12 μm glides gradually while the proportion of flcos with a diameter ranging from 48 to 96 μm and over 96 μm has been increasing gradually with stability. When the shear rate of 21.97 s^{-1} was reached, the proportion of small sediment particles reached the minimum while the proportion of large flocs reached the maximum. If the shear rate elevated further, the flocs with a diameter longer than 48 μm became hard to form while the gliding amplitude of small sediment particles narrowed though the flocculation was still able to occur. The results demonstrated that, for the sediment from the Three Gorges Reservoir, the enhanced shear rate may impel the flocculation of the sediment with small particle sizes under a low turbulence shear rate sustained. When the shear rate was higher than 21.97 s^{-1}, the flocs of big sizes were unable to maintain themselves due to the turbulence with high intensity, which caused the disintegration of flocs to small sediment particles [32].

As shown in Fig. 9a, the tendency of the median diameter of the sediment ascended first and then descended rapidly as the intensity of turbulence increased under different concentrations of the sediment. However, an obvious positive correlation was expressed between the desorption amount of P and the intensity of turbulence, indicating that the dominant factor of the desorption of P is not the particle size of the sediment but the hydrodynamic conditions. The enhanced intensity of turbulence impelled the matter exchange between the sediment and the water, which relatively augmented the diffusion coefficient to further promote the desorption of P from the sediment [33,34]. Subjected to Fig. 9b, two phases of the augmentation of the desorption of P differed obviously from each other. The former phase of P desorption exhibited a slow augmentation before the shear rate achieved 21.97 s^{-1}, while the later phase of P desorption, of which the shear rate was over 21.97 s^{-1}, tended to augment at a faster speed than the former. According to Fig. 9a, when the shear rate was lower than 21.97 s^{-1}, the influence of turbulence on the flocculation of sediment particle was positive, where many small particles tended to flocculate to a floc. When the shear rate was over the 21.97 s^{-1}, the amplified turbulence may become the obstruct to the flocculation which caused the contain of the sediment in small size increasing. The diagram presented that the influence of particle size on the desorption existed. With the contact area between the water and the sediment after plenty of sediment particles have flocculated, the matter was constricted which restricts the desorption amount of P to some degree [35]. When the intensity of turbulence was sustained in a higher level where the floc was hard to form, due to the disintegration of the flocs with big particle size to small particles of the sediment by the turbulence with high intensity, the contact area between the water and the sediment extended which impelled the desorption of P under the effect of turbulence.

4. Conclusions

This research studied the desorption of P from the sediment in the Three Gorges Reservoir under the turbulence condition, and established the correlation between the intensity of turbulence and the diameter of sediment particles as well as the desorption amount of the pollutants by using a set of quasi-uniform turbulence simulation apparatus. The results showed that the secondary pollution to reservoir water was induced by the sediment in the Three Gorges Reservoir, deteriorating the eutrophication in the Reservoir under specified conditions. The desorption flux was different according to the variation of conditions of

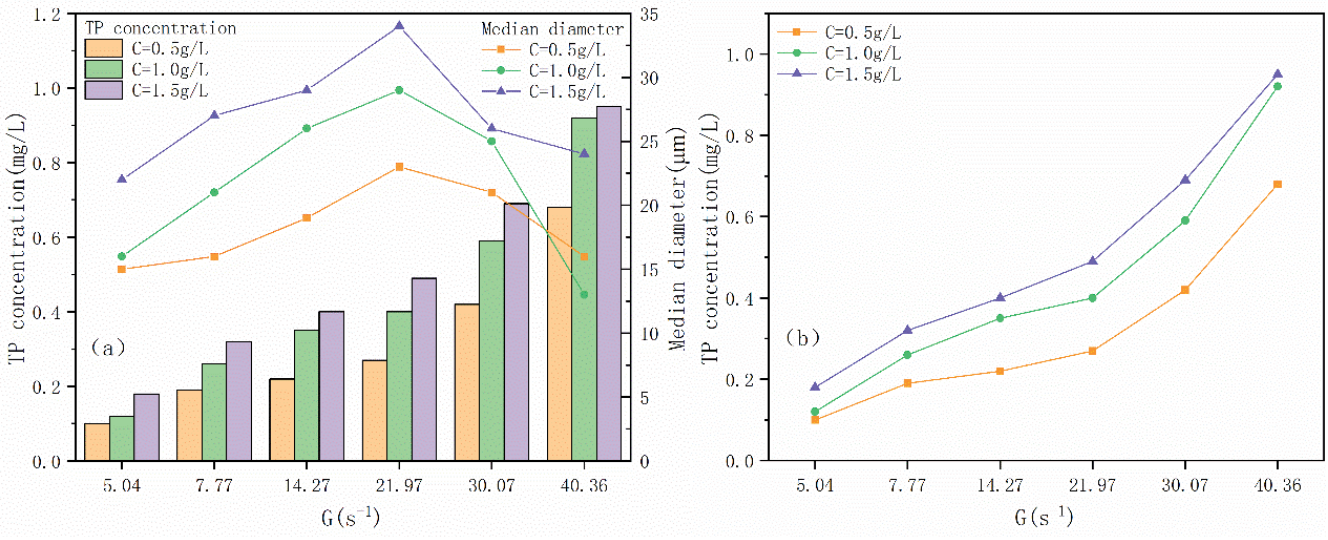

Fig. 9. The desorption of P under the turbulence state.

turbulence, the concentration of the sediment and the temperature. The water with diverse intensities of turbulence could be well simulated quantitatively by adjusting the amplitude and oscillation frequency of approximately even turbulence simulation apparatus. When the intensity was over the critical value, the incipient motion of the bottom sediment was triggered, and a well correlation between the concentration of suspended sediments and intensity of turbulence in water was sustained. As the intensity rose, the incipient motion of the bottom sediment occurred and elevated into water, which caused the release of desorbed P into water. If the intensity of turbulence continued to augment, the concentration of suspended sediments would be higher and the concentration of soluble P would increase quickly. The flocculation of the sediment collected from the Three Gorges Reservoir was able to occur under the turbulence shear rates set in 6 experimental groups. As the intensity of turbulence amplified, the median diameter of the sediment tended to rise first and then to glide with a contrast positive correlation between the desorption amount of P and the intensity of turbulence. The matter exchange between the sediment and the water would be blocked to some degree after the flocculation of the sediment, which could constrict the desorption amount of P to some degree. Moreover, when the intensity of turbulence was at a higher level, the proportion of the sediment of small particle and contact area between the sediment and the water increased, which impelled the desorption of P from the sediment.

Acknowledgments

This work was financially supported by the National Natural Science Foundation of China (Nos. 51609028), the National Natural Science Foundation of Chongqing (Nos. cstc2020jcyj-msxmX0763), the Graduate Research and Innovation Fund of Chongqing (Nos. CYB20180).

Author contributions

Wang Li and Jun Wang conceived and designed the experiments; Wang Li and Jiawen Li performed the experiments; Wang Li and Qingwei Yang conducted data analyses; Bo Zu contributed to the discussion; Wang Li wrote the paper. Wang Li and Bo Zu contributed to the work equally and should be regarded as co-first authors.

Conflicts of interest

The authors declare no conflict of interest.

References

[1] C. Zhang, X.H. Yao, Y. Chen, Q. Chu, Y. Yu, J.H. Shi, H.W. Gao, Variations in the phytoplankton community due to dust additions in eutrophication, LNLC and HNLC oceanic zones, Sci. Total Environ., 669 (2019) 282–293.
[2] X.Y. Wang, Y.Q. Zhou, Z.Y. Zhao, L. Wang, J.P. Xu, J.B. Yu, A novel water quality mechanism modeling and eutrophication risk assessment method of lakes and reservoirs, Nonlinear Dyn., 96 (2019) 1037–1053.
[3] G.Z. Jin, S.-i. Onodera, M. Saito, Y. Shimizu, Sediment phosphorus cycling in a nutrient-rich embayment in relation to sediment phosphorus pool and release, Limnology, 21 (2020) 415–425.
[4] C. Carneiro, P. Kelderman, K. Irvine, Assessment of phosphorus sediment–water exchange through water and mass budget in Passaúna Reservoir (Paraná State, Brazil), Environ. Earth Sci., 75 (2016) 564–572.
[5] H.W. Zhu, D.Z. Wang, P.D. Cheng, J.Y. Fan, B.C. Zhong, Effects of sediment physical properties on the phosphorus release in aquatic environment, Sci. China Phys. Mech. Astron., 58 (2015) 1–8.
[6] P. Yang, Huanghe, R. Gao, Characteristics of phosphorus adsorption and release in different types of sediments, Int. J. Sci. Res. Manage., 8 (2020) 342–354.
[7] Y. Zhang, P. Hei, J. Yang, J. Jin, G. Zhou, Effects of native adsorptive substances on phosphorus adsorption capacity of Yangtze River sediment, Res. Environ. Sci., 30 (2017) 545–551.
[8] Y. Xiao, X.-l. Zhu, H.-k. Cheng, K.-j. Li, Q. Lu, D.-f. Liang, Characteristics of phosphorus adsorption by sediment mineral matrices with different particle sizes, Water Sci. Eng., 6 (2013) 262–271.
[9] P.J.A. Withers, H.P. Jarvie, Delivery and cycling of phosphorus in rivers: a review, Sci. Total Environ., 400 (2008) 379–395.
[10] J.H. Bai, X.F. Ye, J. Jia, G.L. Zhang, Q.Q. Zhao, B.S. Cui, X.H. Liu, Phosphorus sorption-desorption and effects of temperature, pH and salinity on phosphorus sorption in marsh soils from coastal wetlands with different flooding conditions, Chemosphere, 188 (2017) 677–688.
[11] L. Zhang, Y. Du, C. Du, M. Xu, H.A. Loáiciga, The adsorption/desorption of phosphorus in freshwater sediments from buffer zones: the effects of sediment concentration and pH, Environ. Monit. Assess., 188 (2016) 13–20.
[12] J. Qian, K. Li, P. Wang, C. Wang, M. Shen, J. Liu, X. Tian, B. Lu, Effects of carbon nanotubes on phosphorus adsorption behaviors on aquatic sediments, Ecotoxicol. Environ. Saf., 142 (2017) 230–236.
[13] S.-l. Huang, C.-o. Ng, Q.-z. Guo, Experimental investigation of the effect of flow turbulence and sediment transport patterns on the adsorption of cadmium ions onto sediment particles, J. Environ. Sci.-China, 19 (2007) 696–703.
[14] Y.-Q. Ding, G.-W. Zhu, B.-Q. Qin, Y.-P. Wang, T.-F. Wu, X. Shen, D.-L. Hong, Experimental study on the effect of wave disturbances on the phosphorus dynamics in shallow lakes, Adv. Water Sci., 22 (2011) 273–278.
[15] J.P. Peng, Y. Pang, L.I. Yi-Ping, L. Ding, Change of phosphorus in lake after water dynamical condition and its contribution to eutrophication, Ecol. Environ. Sci., 4 (2004) 43–45.
[16] W.A. House, F.H. Denison, P.D. Armitage, Comparison of the uptake of inorganic phosphorus to a suspended and stream bed-sediment, Water Res., 29 (1995) 767–779.
[17] H. Erqing, J. Chunbo, L. Defu, Phosphorus adsorption rule of the suspended silt in the turbulent waterbody, J. Sediment Res., 2 (2009) 34–37.
[18] A.J.S. Cuthbertson, P. Dong, P.A. Davies, Non-equilibrium flocculation characteristics of fine-grained sediments in grid-generated turbulent flow, Coastal Eng., 57 (2010) 447–460.
[19] T.R. Camp, Velocity gradients and internal work in fluid motion, J. Boston Soc. Civ. Eng., 30 (1943) 219–230.
[20] I. Nezu, H. Nakagawa, G.H. Jirka, Turbulence in open-channel flows, J. Hydraul. Eng., 120 (1994) 1235–1237.
[21] L.H. Kalnejais, W.R. Martin, M.H. Bothner, The release of dissolved nutrients and metals from coastal sediments due to resuspension, Mar. Chem., 121 (2010) 224–235.
[22] X.L. Cheng, Y. Huang, X. Pu, R.D. An, W.D. Huang, J. Li, W. Wang, R. Li, Spatial and seasonal distribution and transportation of different forms of phosphorus in the middle reaches of the Yarlung Zangbo River, Water, 10 (2018) 1858–1869.
[23] L. Yang, F. Lin, Z. Xu, M. Zhang, Y. Gao, Effect of temperature on the activities of microorganism and the pollutants release in the bioremediation of the sediment, Environ. Pollut. Control, 29 (2007) 22–29.
[24] K. Zhang, P.-d. Cheng, B.-c. Zhong, D.-z. Wang, Total phosphorus release from bottom sediments in flowing water, J. Hydrodyn. Ser. B, 24 (2012) 589–594.

[25] H. Zhu, J. Jiang, P. Cheng, D. Wang, Mechanism of pollutant release due to sediment re-suspension, Adv. Water Sci., 24 (2013) 537–542.
[26] A. Mhashhash, B.N. Bockelmann-Evans, S.Q. Pan, Effect of hydrodynamics factors on sediment flocculation processes in estuaries, J. Soils Sediments, 18 (2018) 3094–3103.
[27] J.Y. Shang, C.X. Liu, Z.M. Wang, J.M. Zachara, Effect of grain size on uranium(VI) surface complexation kinetics and adsorption additivity, Environ. Sci. Technol., 45 (2011) 6025–6031.
[28] J.-y. Fan, X.-y. He, D.-z. Wang, Experimental study on the effects of sediment size and porosity on contaminant adsorption/desorption and interfacial diffusion characteristics, J. Hydrodyn., 25 (2013) 20–26.
[29] J. Fan, G. Zhao, J. Sun, Binary component sorption of cadmium, and copper ions onto Yangtze River sediments with different particle sizes, Sustainability, 9 (2017) 2089–2102.
[30] B. Xia, Q.H. Zhang, J.S. Yang, C.B. Jiang, Experimental investigation of the effect of flow turbulence on the adsorption of phosphorus onto sediment particles, Appl. Mech. Mater., 212–213 (2012) 299–306.
[31] L. Zhang, C.-X. Fan, J.-J. Wang, C.-H. Zheng, Space-time dependent variances of ammonia and phosphorus flux on sediment-water interface in Lake Taihu, Environ. Sci., 27 (2006) 1537–1549.
[32] D.H. Bache, Floc rupture and turbulence: a framework for analysis, Chem. Eng. Sci., 59 (2004) 2521–2534.
[33] K. Zhang, B. Li, D. Wang, Contaminant (COD_{Cr}) release from river bottom sediments under flow conditions, Acta Scientiae Circumstantiae, 30 (2010) 985–989.
[34] J.Z. Huang, X.P. Ge, X.F. Yang, B. Zhang, D.S. Wang, Remobilization of heavy metals during the resuspension of Liangshui River sediments using an annular flume, Sci. Bull., 57 (2012) 3567–3572.
[35] Z.H. Chai, G.L. Yang, M. Chen, M.H. Yu, The effect of uniform shear flow on flocculation of cohesive fine sediment, J. Hydraul. Eng., 43 (2012) 1194–1201.